JCI The Journal of Clinical Investigation

Aberrant splicing contributes to severe α-spectrin-linked congenital hemolytic anemia

Patrick G. Gallagher, … , Susan J. Baserga, Vincent P. Schulz

J Clin Invest. 2019. https://doi.org/10.1172/JCI127195.

Research In-Press Preview **Genetics** **Hematology**

Graphical abstract

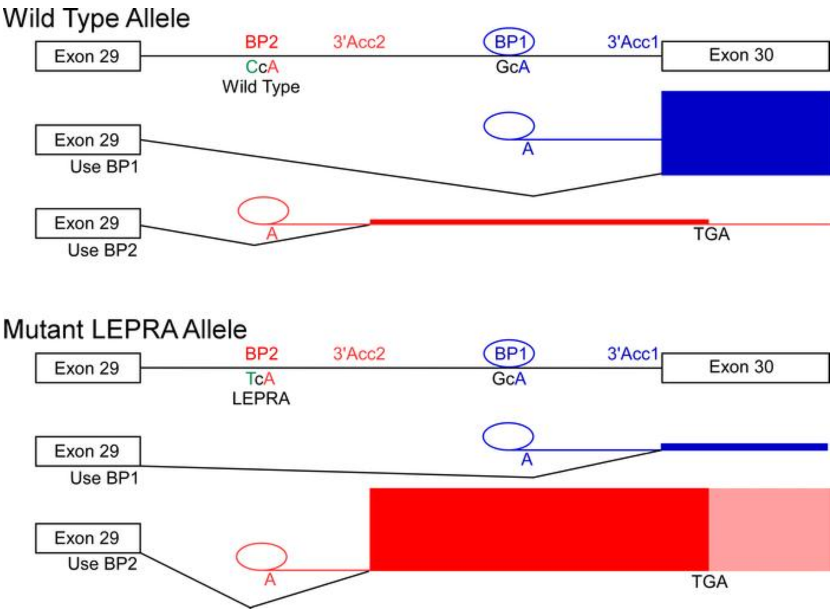

Aberrant splicing contributes to severe α-spectrin-linked congenital hemolytic anemia

Patrick G. Gallagher,[1,2,3] Yelena Maksimova,[1] Kimberly Lezon-Geyda,[1]
Peter E. Newburger,[4] Desiree Medeiros,[5] Robin D. Hanson,[6] Jennifer Rothman,[7] Sara Israels,[8]
Donna A. Wall,[9] Robert F. Sidonio, Jr.,[10] Colin Sieff,[11] L. Kate Gowans,[12] Nupur Mittal,[13]
Roland Rivera-Santiago,[14] David W. Speicher,[14] Susan J. Baserga,[2,15] Vincent P. Schulz[1]

[1]Department of Pediatrics, Yale University School of Medicine, New Haven, CT 06520, USA; [2]Departments of Genetics, Yale University School of Medicine, New Haven, CT 06520, USA; [3]Department of Pathology, Yale University School of Medicine, New Haven, CT 06520, USA; [4]Department of Pediatrics, University of Massachusetts Medical School, Worcester, MA 01655, USA; [5]Kapiolani Medical Center for Women & Children, Honolulu, HI 96826, USA; [6]Cardinal's Kids Cancer Center, St. Louis, MO 63141, USA; [7]Department of Pediatrics, Duke University Medical Center, Durham, NC 27708, USA; [8]Department of Pediatrics and Child Health, University of Manitoba, Winnipeg, MB, R3E 0V9, Canada; [9] Hospital for Sick Children, University of Toronto, Toronto ON M5G1X8, Canada, [10]Department of Pediatrics, Emory University School of Medicine, Atlanta, GA 30322, USA; [11]Harvard Medical School, Dana-Farber and Boston Children's, Cancer and Blood Disorders Center, Boston, MA 02215, USA; [12]Beaumont Children’s Hospital, Royal Oak, MI 48073, USA; [13]Department of Pediatrics, Rush University Medical Center, Chicago, IL 60612, USA. [14]The Center for Systems and Computational Biology and Molecular and Cellular Oncogenesis Program, The Wistar Institute,

Philadelphia, PA, 19104, USA; [15]Departments of Molecular Biophysics and Biochemistry and Therapeutic Radiology, Yale University School of Medicine, New Haven, CT 06520, USA.

Running Title: Aberrant Branch Point and Severe Anemia

The authors have declared that no conflicts of interest exist.

Address correspondence to: Patrick G. Gallagher, Department of Pediatrics, Yale University School of Medicine, 333 Cedar Street, P. O. Box 208064, New Haven, CT 06520-8064. Tel: (203) 688-2896; Fax: (203) 785-6974; Email: patrick.gallagher@yale.edu

Abstract

The etiology of severe hemolytic anemia in most patients with recessive hereditary spherocytosis (rHS) and the related disorder hereditary pyropoikilocytosis (HPP) is unknown. Whole exome sequencing of DNA from probands of 24 rHS or HPP kindreds identified numerous mutations in erythrocyte membrane α-spectrin (*SPTA1).* Twenty-eight mutations were novel, with null alleles frequently found in *trans* to missense mutations. No mutations were identified in a third of *SPTA1* alleles (17/48). Whole genome sequencing revealed linkage disequilibrium between the common rHS-linked α-spectrin$^{\text{Bug Hill}}$ polymorphism and a rare intron 30 variant in all 17 mutation-negative alleles. In vitro minigene studies and in vivo splicing analyses revealed the intron 30 variant changes a weak alternate branch point (BP) to a strong BP. This change leads to increased utilization of an alternate 3'splice acceptor site, perturbing normal α-spectrin mRNA splicing and creating an elongated mRNA transcript. In vivo mRNA stability studies revealed the newly created termination codon in the elongated transcript activates nonsense mediated decay leading to spectrin deficiency. These results demonstrate a unique mechanism of human genetic disease contributes to the etiology of a third of cases of rHS, facilitating diagnosis and treatment of severe anemia, and identifying a new target for therapeutic manipulation.

Introduction

Hereditary spherocytosis (HS), the most common inherited hemolytic anemia in Northern Europeans, affects people of every ethnic background worldwide. A quarter of HS cases exhibit recessive inheritance (rHS).(1-5) Clinically, rHS patients are more severely affected than patients with typical, dominant HS, often presenting in infancy or early childhood with life-threatening, hemolytic anemia.(1, 2, 5) Many of these patients are transfusion-dependent. Erythrocyte membranes from patients with rHS and the related disorder HPP are spectrin-deficient which leads to destabilization of the lipid bilayer.(1, 2, 5-7) The degree of spectrin deficiency correlates with the degree of hemolysis and the clinical response to splenectomy.(6) Biochemical and genetic studies have implicated defects of α spectrin in most rHS and HPP patients, but in most, the molecular basis of disease is unknown.(1, 5, 7-9)

In normal erythroid cells, α spectrin is synthesized in large excess, with α spectrin synthesized in excess of β spectrin by a 3-4:1 ratio.(10-12) Thus patients with one normal and one production-defective defective α-spectrin allele are biochemically and clinically normal, because normal α-spectrin production remains in excess and normal amounts of αβ spectrin heterodimers are assembled on the membrane. Patients who are homozygotes or compound heterozygotes for defects of α-spectrin production will suffer from rHS.(13) Similarly, patients who are compound heterozygotes for a structurally defective α-spectrin allele and a defective α-spectrin production allele will suffer from HPP.(8, 9, 14)

We have studied the genetic basis of α-spectrin linked anemia in 24 kindreds with rHS or HPP, including the first α-spectrin deficient rHS kindreds described by Agre *et al*.,(1, 2, 15) as well as a group of transfusion dependent patients, using whole exome sequencing. We identified numerous novel mutant α-spectrin (*SPTA1*) alleles, including null alleles and missense mutations, primarily in the αβ-spectrin self-association site. In 17 of 48 alleles, only one or no deleterious *SPTA1* mutations were identified. Whole genome sequencing of selected individuals identified the α^{LEPRA} allele, a rare, poorly characterized variant identified in a patient with rHS associated with an elongated α-spectrin mRNA transcript,(13) *in trans* to other mutations. Because wild type erythroid cells also carry the elongated transcript described with the α^{LEPRA} allele, its role in the pathogenesis of α-spectrin deficiency and inherited anemia has been unclear.

In a series of in vitro minigene splicing studies and in vivo splicing assays, we demonstrate that the α^{LEPRA} variant changes a weak alternate branch point (BP) to a strong BP. This change leads to increased utilization of an alternate 3'splice acceptor site, perturbing normal α-spectrin mRNA splicing and creating the elongated mRNA transcript. In vivo mRNA stability studies in erythroid cells rendered homozygous for the α^{LEPRA} variant via CrispRCas9-based gene editing revealed a newly created termination codon in the elongated transcript activates nonsense mediated decay leading to spectrin deficiency. These studies indicate a novel mechanism of human genetic disease contributes to the etiology of a third of cases of rHS, facilitating disease diagnosis and treatment, and identifying a new target for therapeutic manipulation.

Results

Individuals from 24 kindreds from 3 groups with inherited hemolytic anemia were studied using whole exome sequencing. One group was individuals from 5 spectrin-deficient rHS kindreds from the original reports of HS by Agre *et al.*(1, 2, 15) and 2 spectrin-deficient rHS kindreds described by Tse *et al.*(3) Clinical and laboratory details of these patients have been previously described. A second group was from 7 kindreds with the clinical diagnosis of rHS or HPP referred to the Yale Center for Blood Disorders (YCBD). Clinical and laboratory details of these patients are provided in Supplemental Table S1. The unifying features of this group are that the patients had severe hemolytic anemia and their erythrocyte membranes were spectrin-deficient. The third group was composed of 10 patients from 9 kindreds with transfusion-dependent (TD) anemia referred to the YCBD. Clinical details of these patients are provided in Supplemental Table S2. Prenatal onset of severe hemolytic anemia or onset in the immediate neonatal period, requiring *in utero* or early postnatal transfusion therapy, respectively, were common. All TD patients required chelation for early onset iron overload. Two patients in this group died. One died from complications of anemia in the neonatal period, while its similarly affected sibling remains transfusion dependent. The other patient died from hepatic complications of transfusion-related iron overload at 17 months of age.

Whole exome sequencing identified numerous mutations in α-spectrin (*SPTA1)*, with 28 of 48 alleles carrying novel variants (Table 1). No deleterious mutations were identified in other erythrocyte membrane protein genes. Null *SPTA1* alleles were frequently found in *trans* to missense mutations. Two TD patients had deleterious mutations in both *SPTA1* alleles; one with nonsense mutations in *trans* died of liver failure associated with iron overload (patient 16), the other with nonsense and splicing mutations in *trans* remains transfusion dependent. Six missense mutations were identified, with 4 in the αβ-spectrin self-association site, critical for membrane stability. Modeling studies predicted three mutations (R45G, L49R, R28H) disrupt tetramer formation while a fourth, M70R, although not directly located in the tetramer interface, creates steric hindrance with the laterally associated spectrin chain in bivalent tetramers (Supplemental Figures S1 and S2). One TD kindred patient homozygous for the R45G mutation had a sibling homozygous for the same mutation die in the immediate perinatal period due to complications of anemia (patient 21).

In 17 of 48 alleles, no deleterious mutations were identified. All 17 alleles carried the common α-spectrin$^{\text{Bug Hill}}$ polymorphism, (rs35948326,NM_003126.2:c.2909C>A, NP_003117.2:p.Ala970Asp, α^{BH}), previously associated with α-spectrin-linked rHS (Supplemental Figure S3).(3) Whole genome sequencing of two rHS patients heterozygous for the α^{BH} variant was performed. Comparison to samples in the 1000 Genomes database revealed a single, common *SPTA1* variant, α^{LEPRA}, chr1:158613314C>T, present on only 4 of 4610 alleles in 1000 Genomes. In all 4, it was heterozygous and in *cis* to the α^{BH} allele. This rare intron 30 variant was previously described in a rHS patient in *trans* to a *SPTA1* nonsense mutation.(13) Analysis of α^{BH} haplotypes revealed 3 predominant patterns (Figure 1) with the haplotype of the rHS patients identical to the 4 heterozygous α^{LEPRA} individuals. All 17 mutation-negative alleles carried the α^{LEPRA} mutation, in *trans* to other mutations in 16 patients (Table 1). The proband lacking any deleterious *SPTA1* alleles was homozygous for the α^{LEPRA} allele. Thus, a third of all mutant *SPTA1* alleles associated with severe hemolytic anemia carried the α^{LEPRA} variant.

In the original description of the α^{LEPRA} variant, RT-PCR of reticulocyte RNA demonstrated the α^{LEPRA} allele was associated with an elongated α-spectrin mRNA transcript.(13) This transcript contained 70nt from the 3’ end of intron 30 and was predicted to lead to frameshift and premature chain termination.(13) Located 29nt upstream of the alternate acceptor splice, it was unclear if or how the α^{LEPRA} variant influenced α-spectrin pre-mRNA splicing. Examination of this region in transcriptomes derived from RNA-seq of primary human wild type (WT) erythroid cells at varying stages of development and differentiation reveals that an alternately spliced, elongated transcript identical to that associated with α^{LEPRA} is produced on the background of WT *SPTA1* alleles, ranging from 2.4 to 6.8% of total α-spectrin transcripts (Figure 2). K562 cells, which do not carry the α^{LEPRA} variant, also produce this transcript. Because WT erythroid cells carry the same elongated transcript described with the α^{LEPRA} allele, its role in the pathogenesis of α-spectrin deficiency and inherited anemia has been unclear, with some speculating it is a single nucleotide polymorphism of no functional importance.

Attempts to quantitate the elongated α-spectrin transcript in reticulocyte RNA from affected patients led to inconsistent results between patients and controls, and between individual samples from the same patient, with elongated/WT α-spectrin mRNA ratios ranging from 3.8-5.4% for controls and 3.5-9.7% for heterozygous α^{LEPRA} patients (not shown). This variability is likely multifactorial, reflecting variability of the contribution of the mutant *SPTA1* allele in *trans* (nonsense, splicing, other mutations) due to mRNA stability, instability of the elongated mRNA transcripts, variability in amounts and differentiation stages of circulating reticulocyte mRNA (early vs. late) in individual patients, shipping-induced changes in mRNA, and limitations of PCR-based assays.

To gain insight into potential effects of the α^{LEPRA} allele on mRNA processing, a series of bioinformatic studies were performed. Analysis of *SPTA1* intron 30 using Sroogle, which analyzes splicing signals and the influence of mutations on splicing,(16) predicted: 1) a branch point (BP1) at the expected location 31bp 5’ of the 3’ acceptor site (3’Acc1) of exon 31; 2) an alternate upstream BP centered on an “A” 2bp 3’ of the α^{LEPRA} mutation (BP2); 3) a novel alternate 3’ acceptor site downstream of BP2 (3’Acc2); and 4) the α^{LEPRA} variant significantly improves the probability of using BP2 (Schematic in Figure 3A/B). These findings predict alternate BP usage between wild type and α^{LEPRA} alleles influences transcript composition and abundance. The algorithm Branchpointer, an algorithm that predicts and analyzes BP,(17) indicated WT BP1 and BP2 have low BP probability scores (0.51 and 0.67, respectively), while the α^{LEPRA} variant markedly improves the probability score of BP2 (0.94, Figure 3C), supporting the Sroogle predictions. These observations are true when comparing intron 30 BP probability scores to predicted BPs of 8180 introns of 1000 highly expressed erythroid genes (Figure 3D).

To experimentally validate the bioinformatic predictions, functional analyses were performed in minigene assays, a valuable technique for study of splicing,(18-20) and in cells manipulated via CRISPR/Cas9-based gene editing. A set of minigenes with mutation of predicted splicing elements on the background of WT and α^{LEPRA} alleles were analyzed in K562 cells (Figure 4). A WT minigene yielded only 0.78% of the elongated α-spectrin transcript (from use of BP2). In contrast, a minigene containing the α^{LEPRA} mutation yielded 42% of the elongated transcript. To address the critical question of whether BP2 is a functional BP, we mutated the invariant “A” of BP2 to “G” (Figure 4). This minigene yielded 100% WT and no elongated α-spectrin mRNA transcript.

To address the critical question of whether BP2 is a functional BP, we mutated the invariant “A” of BP2 to “G” (Figure 4). This minigene yielded 100% WT and no elongated α-spectrin mRNA transcript. To further validate BP2 as a functional BP, we created K562 cells homozygous for “G” in BP2 (from central “A”) using gene editing. Mutation of BP2 “A” also eliminated the elongated α-spectrin mRNA transcript (Supplemental Data). These data support the prediction that BP2 is a functional BP.

Additional aspects of α-spectrin mRNA processing were also assessed (Figure 4). Mutation of the alternate 3’ splice acceptor site led to abolition of the elongated transcript. Changing the poor BP consensus of BP1 to a U2 binding consensus sequence(21) yielded 100% WT and no elongated α-spectrin transcript. These studies indicate the α^{LEPRA} mutation, located upstream of an alternate 3’ splice acceptor site, changes a weak alternate BP to a strong BP (BP2) in the context of a poor primary BP (BP1). These changes lead to increased usage of the alternate 3’splice acceptor site, which is utilized at a low amount in WT cells, creating an alternate elongated α-spectrin mRNA transcript that leads to frameshift and a novel termination codon.

The novel termination codon, 87nt upstream of an exon-exon junction, is in a position predicted to activate nonsense mediated decay (NMD).(22, 23) To address whether NMD of the elongated transcript is the mechanism of α-spectrin deficiency, we created K562 cells homozygous for the α^{LEPRA} allele using gene editing (Supplemental Data) and treated them with NMD inhibitors emetine or cycloheximide.(24, 25) In homozygous α^{LEPRA} and to a lesser extent in WT cells, the total amount of elongated transcript increased relative to total alpha Spectrin transcript after NMD inhibition (Figure 5A).

To further validate these observations, we inserted 2nt into the polypyrimidine tract of the 3’splice acceptor site of exon 30 (3’Acc1), putting the elongated transcript in-frame in our minigene model. On both WT and α^{LEPRA} backgrounds, the amount of the elongated α-spectrin transcript increased (Figure 5B) supporting the conclusion NMD is responsible for low levels of α-spectrin mRNA associated with utilization of BP2.

Discussion

Mutations leading to alterations in normal mRNA splicing are a major cause of genetic disease.(26-28) Most are *cis*-acting mutations located in canonical donor or acceptor splice site sequences, with others in proteins involved in the splicing process.(26, 28) Only a small number of *cis* mutations in BP consensus sequences have been reported, associated with mutation or deletion of the canonical "A" or mutation of the -2"U".(29, 30) With α^{LEPRA}, strengthening of an alternate BP in the appropriate *cis*-context creates a series of aberrant splicing events that lead to decreased amount of normal mRNA transcripts. As shown here, application of whole genome sequencing to the study of inherited disorders is expected to increase the number of disease-associated intronic mutations influencing splicing, including abnormalities of intronic BPs.(31)

These studies identify a novel mechanism of disease and reveal the etiology underlying many cases of rHS, HPP and TD anemia. They also resolve an unanswered question of the role of the α^{LEPRA} allele in cases of severe anemia where its contribution to α-spectrin deficiency and disease pathogenesis had been unknown. (13, 32-35) Correlating genotype with erythrocyte α-spectrin protein amounts determined by radioimmunoassay, a patient homozygous for the α^{LEPRA} allele exhibited 59% α-spectrin protein on the membrane and a compound heterozygote with α^{LEPRA} in trans to a null allele exhibited 34% to α-spectrin protein on the membrane.(1, 2) This leads to speculation that α^{LEPRA} allele spectrin deficiency is associated with ~30% of normal α-spectrin protein assembled on the mature erythrocyte membrane.

These data demonstrate significant genetic heterogeneity in α-spectrin-linked hemolytic anemia supporting the use of genomic strategies for disease diagnosis, particularly in severe and TD cases. These observations will facilitate disease diagnosis, as most diagnostic gene panels for hereditary hemolytic anemias do not include the intronic region containing the α^{LEPRA} variant nor do most whole exome sequencing capture panels.

When identified in affected patients, the findings are actionable, allowing design of appropriate therapy. In our cohort, 3 patients have become transfusion independent after splenectomy and 2 have become transfusion independent after hematopoietic stem cell transplant.

The α^{LEPRA} allele is a new target for therapeutic gene manipulation.(26, 36-38) Therapies targeting splicing, particularly antisense oligonucleotides which recognize *cis* RNA regulatory elements and alter splicing or target transcripts for degradation and small molecule-based strategies that target splicing factors or RNA sequences and/or RNA structure, are showing significant promise.(26, 36) The α^{LEPRA} allele is also an attractive candidate for therapeutic gene editing, as our data indicate alteration of the α^{LEPRA} allele variant itself or the alternate 3'acceptor site will abolish production of the mutant, elongated α-spectrin mRNA transcript.

The data demonstrate how the synthesis of complementary lines of investigation, clinical, laboratory, biochemical and genetic data, can be leveraged to define and advance our understanding, diagnosis, and treatment of inherited disease.

Methods

Erythrocyte membrane preparation, quantitation of spectrin content and limited tryptic digestion of spectrin. Erythrocyte membranes were prepared from peripheral blood as previously described.(39) Membrane proteins were analyzed and spectrin content determined as described.(40) Membrane proteins were separated by sodium dodecyl-sulfate-polyacrylamide gel electrophoresis (SDS-PAGE) on 3.5% -17% gradient polyacrylamide gels and stained with Coomassie blue. The spectrin/band 3 ratio was quantified by densitometric scanning of the stained gels at 540nm and integration of the surface area under the spectrin and band 3 peaks.(41) Spectrin was extracted by incubating ghosts overnight at 4°C in low ionic strength buffer. Limited tryptic digests of spectrin extracts were prepared as described(39) and separated by two-dimensional gel electrophoresis with isoelectric focusing (IEF) as modified by Speicher *et al*.(42)

Exon capture and whole exome sequencing (WES). Targeted regions of genomic DNA were captured using a SeqCap EZExome V2.0 (Roche) solution-based capture system according to the manufacturer’s protocol. The captured, purified and amplified libraries targeting exomes from patients were sequenced on a HiSeq Analyzer with paired-end sequencing at 75bp read length. Sequencing reads were processed and analyzed as described.[8]

Fastq sequence reads were aligned to the human genome (hg19build37/GRCh37) using BWA mem 0.7.9a software.[9] Variant analysis was performed using Genome Analysis Toolkit (GATK) analysis software v.3.1-1.[10,11] Sequencing reads in the region of known insertion/deletions in the 1000 genomes database were realigned to reduce false positive variants. Individual base quality scores were empirically recalibrated using covariate information in combination with the variation in dbSNP build 137 SNP's and from 629 human genome sequences from the 1000 Genomes project.[12,13] Base alignment quality scores were determined then recalibrated with GATK to further reduce false positive calls.[14] SNP's and indels were called using the GATK HaplotypeCaller Bayesian algorithm for variant discovery and genotyping which uses base qualities and allele counts to determine probabilities for called variants. Indels and novel SNPs were annotated using Annovar,(43) which determines if a SNP or indel changes a protein sequence or splice site, and provides a variety of predictions (including the Combined Annotation Dependent Depletion (CADD) algorithm(44) and Mutation Taster(45)) to assess the likely effect of a mutation on protein function.

Whole genome sequencing (WGS). Genomic DNA was prepared using the TruSeq PCR-free DNA HT sample preparation kit (Illumina) with 450bp insert size. Intact genomic DNA was sheared, followed by end-repair and bead-based size selection of fragmented molecules. Adenines were added to the 3’ ends of the DNA size-selected fragments followed by ligation of Illumina sequence adaptors ligated onto the fragments and PCR. Library quality control included a measurement of the average size of library fragments using a BioAnalyzer (Agilent), estimation of the total concentration of DNA by PicoGreen (Thermo Fischer Scientific), and a measurement of the yield and efficiency of the adaptor ligation process via a quantitative PCR assay using primers specific to the adaptor sequence.

Sequencing was performed on a HiSeq X instrument (Illumina) generating 2x150bp read lengths. After alignment and duplicate removal, this equated to 30x mean genome coverage (for the gender specific ~2.85Gb mappable human genome). WGS data was processed through an automated pipeline at New York Genome Center’s high-performance computational facility. Paired-end 150bp reads from the WGS were aligned to the GRCh37 human reference using the Burrows-Wheeler Aligner (BWA-MEM v0.78)(46) and processed using the best-practices pipeline that includes marking of duplicate reads by the use of Picard tools (v1.83, http://picard.sourceforge.net), realignment around indels, and base recalibration via GATK v3.2.2.(47)

Two patients (# 1, #23) were selected for whole genome sequencing (WGS), both heterozygous for the $\alpha^{\text{Bug Hill}}$ variant. Analyzing WGS data, 122 variants in the *SPTA1* region (chr1:158545000-158690000) present in both samples were selected for further analysis using Annovar software to annotate allele frequencies and predicted functional consequences. In addition, we identified samples in the 1000 Genomes database of healthy individuals that were homozygous for $\alpha^{\text{Bug Hill}}$ and downloaded genotype data for these individuals. Variants present in the two patient samples that were homozygous in the 1000 Genomes samples were excluded from further analysis, leaving 16 candidate variants, of which 4 were excluded because they were present at high frequency (>1%) in the 1000 Genomes database. Eleven remaining variants were excluded because they were homopolymeric or short tandem repeat size variations that are common and often not accurately genotyped. The sole remaining variant, rs200830867, chr1:158613314 G to A, is the α^{LEPRA} allele.(13) This variant was initially described in an rHS patient in *trans* to an *SPTA1* nonsense mutation associated with an elongated α-spectrin mRNA transcript containing 70nt from the 3’ end of intron 30 hypothesized to lead to frameshift and premature chain termination.(13)

Mutation validation. Variants identified by whole exome or whole genome sequencing were validated by Sanger sequencing. Sanger sequencing was performed on an 3130XL capillary sequencer (Applied Biosystems). *SPTA1* variants were classified as *cis* or *trans* by study of the proband’s parents. Variants were classified as novel if not found in the 1000G or ExAc databases.

Molecular modeling. The effects of α-spectrin missense mutations on tetramer structure and their likely functional consequences were evaluated using the structures of the univalent α-β tetramer complex,(48) closed spectrin dimers,(49, 50) and the divalent tetramer complex as templates.(50)

Minigene analyses. Minigene splicing assays were designed as described.(18) Plasmids were constructed containing the human erythroid *ANK1* promoter, the human *HBG1* gene including the *HBG1* ATG/Kozak consensus, and the region of the *SPTA1* gene containing either WT or α^{LEPRA} sequence for use in minigene splicing assays. Briefly, a SmaI-BglII fragment of the *ANK1* gene promoter was linked to a BglII-HindIII fragment containing exons 1-3 of the *HBG1* gene and flanking 3' region. A 1684bp XbaI fragment of the *SPTA1* gene from intron 29 to intron 32, containing either the WT or α^{LEPRA} sequence, was cloned into intron 2 of the *HBG1* gene. These plasmids contained a termination codon and the polyadenylation signal from the *HBG1* gene.

Wild-type and α^{LEPRA} spectrin minigene plasmids containing fragments of the *SPTA1* gene from intron 29 to intron 32 were prepared and transfected into 10^7 K562 cells (ATCC CCL-243) using nucleofection program T-016, buffer V (Amaxa). Cells were harvested after 48 hours, RNA was prepared, then reverse transcribed using oligo d(T) and random hexamers, then cDNA was amplified with primers that include sequence from flanking *HBG1* and internal *SPTA1* exons. These primers allow differentiation of minigene amplification products from endogenous *SPTA1* transcripts.

Fluorescent Taqman probes (Applied Biosystems) corresponding to total *SPTA1* and the elongated α-spectrin transcript were added to amplification reactions, allowing determination of the contribution of elongated α-spectrin transcripts after normalization. To assay total minigene

SPTA1 transcript, PCR was performed using primers 5'-CTTGGAGACTATGCCAACCTAAA-3' (sense) and 5'-CACATTTCCCAGGAGCTGAA-3' (antisense) with transcript quantitation by Taqman probe 5'-AATGGATCAGTGAGATGCTGCCCA-3' (sense). To assay elongated α-spectrin transcripts, PCR was performed using primers G4833, 5'-GAGAATTCCCTGAGGTCAGATG-3'-(sense) and G44820, 5'-ATCCCAGACTCCCTCCTG-3' (antisense) with transcript quantitation by Taqman probe 5'-AGGCTTTGATGAAGAAACGGGACGA-3' (sense). All analyses included 3 biologic and 2 technical replicates.

CRISPR/Cas9 gene editing analyses. Four guide RNAs in the regions flanking the predicted BP2/α^{LEPRA} region were designed, synthesized and tested for use in gene editing experiments. gRNAs were synthesized using HiScribe™ T7 High Yield RNA Synthesis Kit (New England Biolabs). Testing was done using Guide-it™ sgRNA Screening Kit (Takara). One gRNA was selected and used for all experiments (Target sequence: GGATTCAGAAGATATACTCA). Fifteen micrograms of Cas9 protein (PNAbio) was complexed with 200pmoles of gRNA. The gRNA-Cas9-RNP complex and 200 pmoles of donor ssDNA [BP2 "A" to "G" donor ssDNA: g(s)g(s)a(s)actctgtaccacacaagtagcccattattagatgtttctcctcctattaagttgaaacccacctccctgtaaggcatatattatttgaccctgagtatatcttctgaatccGcaaaggataccttt(s)c(s)a(s) or α^{LEPRA} donor ssDNA: g(s)g(s)a(s)actctgtaccacacaagtagcccattattagatgtttctcctcctattaagttgaaacccacctccctgtaaggcatatattatttgaccctgagtatatcttctgaatTcacaaaggataccttt(s)c(s)a(s)] were nucleofected (Amaxa) into K562 cells using T-016 nucleofector program. Cells were placed into 96 well plates 48 hours post nucleofection. Clones were expanded 10-14 days, and then screened for either homozygous substitution of the BP2 "A" to "G" or homozygous alteration of the wild type nucleotide the

α^{LEPRA} substitution “C” to “T” by PCR amplification followed by Sanger nucleotide sequencing. Homozygous mutant BP2 and α^{LEPRA} clones were identified and used in additional studies (Supplemental Figure S4).

mRNA stability assays. The influence of nonsense mediated decay (NMD) on the stability of WT α-spectrin and α^{LEPRA} mRNA was examined in WT K562 cells and in K562 cells rendered homozygous for the α^{LEPRA} allele. Cells were incubated at 37^{o}C with the NMD inhibitor emetine (100ug/ml, emetine dihydrochloride hydrate, Sigma, E2375) for 8 hours or with the NMD inhibitor cycloheximide (100ug/ml, Sigma, C1988) for 4 hours, or with a combination of both. The amount of total α-spectrin mRNA transcripts and α^{LEPRA} mRNA transcripts were determined by real time RT-PCR with fluorescent probes as described above. Analyses included 3 biologic and 3 technical replicates.

Statistics. GraphPad Prism 8 software (Graph Pad Software) was used for statistical analyses. All data were reported as mean +/- sample standard deviation in tables or as error bars. Comparisons between two groups were performed using two-tailed Student’s t test. Multiple test correction was performed using the Benjamini and Hochberg method.(51) Significance was set at p-value <0.05.

Human subjects. All human studies were approved by the Yale University Human Investigation Committee review board. Written informed consent was received from participants or their parents, as appropriate, prior to inclusion in the study.

Author contributions: PGG designed experiments, analyzed data and wrote the manuscript; KLG and YM designed and performed experiments; PEN, DM, RDH, JR, SI, DW, RFS Jr., CS, LKG and NM phenotyped, diagnosed and collected additional information on patients; RRS, DWS, SJB and VPS designed experiments and analyzed data.

Acknowledgements

We thank all patients and their family members for participation. Supported in part by grants from the National Institutes of Health, HL65448, DK106857, DK032094, CA009171, GM115710 and GM122926 and the Arnold J. Alderman family. We dedicate this report to the late Bernard G. Forget.

References

1. Agre P, Orringer EP, and Bennett V. Deficient red-cell spectrin in severe, recessively inherited spherocytosis. *N Engl J Med.* 1982;306(19):1155-61.
2. Agre P, Casella JF, Zinkham WH, McMillan C, and Bennett V. Partial deficiency of erythrocyte spectrin in hereditary spherocytosis. *Nature.* 1985;314(6009):380-3.
3. Tse WT, Gallagher PG, Jenkins PB, Wang Y, Benoit L, Speicher D, et al. Amino-acid substitution in alpha-spectrin commonly coinherited with nondominant hereditary spherocytosis. *Am J Hematol.* 1997;54(3):233-41.
4. Mohandas N. Inherited hemolytic anemia: a possessive beginner's guide. *Hematology Am Soc Hematol Educ Program.* 2018;2018(1):377-81.
5. Gallagher PG. Abnormalities of the erythrocyte membrane. *Pediatr Clin North Am.* 2013;60(6):1349-62.
6. Chasis JA, Agre P, and Mohandas N. Decreased membrane mechanical stability and in vivo loss of surface area reflect spectrin deficiencies in hereditary spherocytosis. *J Clin Invest.* 1988;82(2):617-23.
7. Zarkowsky HS, Mohandas N, Speaker CB, and Shohet SB. A congenital haemolytic anaemia with thermal sensitivity of the erythrocyte membrane. *Br J Haematol.* 1975;29(4):537-43.
8. Gallagher PG, Tse WT, Coetzer T, Lecomte MC, Garbarz M, Zarkowsky HS, et al. A common type of the spectrin alpha I 46-50a-kD peptide abnormality in hereditary elliptocytosis and pyropoikilocytosis is associated with a mutation distant from the proteolytic cleavage site. Evidence for the functional importance of the triple helical model of spectrin. *J Clin Invest.* 1992;89(3):892-8.
9. Costa DB, Lozovatsky L, Gallagher PG, and Forget BG. A novel splicing mutation of the alpha-spectrin gene in the original hereditary pyropoikilocytosis kindred. *Blood.* 2005;106(13):4367-9.
10. Hanspal M, Hanspal JS, Kalraiya R, Liu SC, Sahr KE, Howard D, et al. Asynchronous synthesis of membrane skeletal proteins during terminal maturation of murine erythroblasts. *Blood.* 1992;80(2):530-9.
11. Hanspal M, and Palek J. Biogenesis of normal and abnormal red blood cell membrane skeleton. *Semin Hematol.* 1992;29(4):305-19.
12. Hanspal M, and Palek J. Synthesis and assembly of membrane skeletal proteins in mammalian red cell precursors. *J Cell Biol.* 1987;105(3):1417-24.
13. Wichterle H, Hanspal M, Palek J, and Jarolim P. Combination of two mutant alpha spectrin alleles underlies a severe spherocytic hemolytic anemia. *J Clin Invest.* 1996;98(10):2300-7.

14. Hanspal M, Hanspal JS, Sahr KE, Fibach E, Nachman J, and Palek J. Molecular basis of spectrin deficiency in hereditary pyropoikilocytosis. *Blood.* 1993;82(5):1652-60.
15. Agre P, Asimos A, Casella JF, and McMillan C. Inheritance pattern and clinical response to splenectomy as a reflection of erythrocyte spectrin deficiency in hereditary spherocytosis. *N Engl J Med.* 1986;315(25):1579-83.
16. Schwartz S, Hall E, and Ast G. SROOGLE: webserver for integrative, user-friendly visualization of splicing signals. *Nucleic Acids Res.* 2009;37(Web Server issue):W189-92.
17. Signal B, Gloss BS, Dinger ME, and Mercer TR. Machine learning annotation of human branchpoints. *Bioinformatics.* 2018;34(6):920-7.
18. Cooper TA. Use of minigene systems to dissect alternative splicing elements. *Methods.* 2005;37(4):331-40.
19. Edelman EJ, Maksimova Y, Duru F, Altay C, and Gallagher PG. A complex splicing defect associated with homozygous ankyrin-deficient hereditary spherocytosis. *Blood.* 2007;109(12):5491-3.
20. Wong MS, Kinney JB, and Krainer AR. Quantitative Activity Profile and Context Dependence of All Human 5' Splice Sites. *Mol Cell.* 2018;71(6):1012-26.e3.
21. Pascolo E, and Seraphin B. The branchpoint residue is recognized during commitment complex formation before being bulged out of the U2 snRNA-pre-mRNA duplex. *Mol Cell Biol.* 1997;17(7):3469-76.
22. Kurosaki T, and Maquat LE. Nonsense-mediated mRNA decay in humans at a glance. *J Cell Sci.* 2016;129(3):461-7.
23. Popp MW, and Maquat LE. Leveraging Rules of Nonsense-Mediated mRNA Decay for Genome Engineering and Personalized Medicine. *Cell.* 2016;165(6):1319-22.
24. Conboy JG. RNA splicing during terminal erythropoiesis. *Curr Opin Hematol.* 2017;24(3):215-21.
25. Pimentel H, Parra M, Gee S, Ghanem D, An X, Li J, et al. A dynamic alternative splicing program regulates gene expression during terminal erythropoiesis. *Nucleic Acids Res.* 2014;42(6):4031-42.
26. Scotti MM, and Swanson MS. RNA mis-splicing in disease. *Nat Rev Genet.* 2016;17(1):19-32.
27. Sterne-Weiler T, and Sanford JR. Exon identity crisis: disease-causing mutations that disrupt the splicing code. *Genome Biol.* 2014;15(1):201.
28. Chabot B, and Shkreta L. Defective control of pre-messenger RNA splicing in human disease. *J Cell Biol.* 2016;212(1):13-27.

29. Bishop DF, Schneider-Yin X, Clavero S, Yoo HW, Minder EI, and Desnick RJ. Congenital erythropoietic porphyria: a novel uroporphyrinogen III synthase branchpoint mutation reveals underlying wild-type alternatively spliced transcripts. *Blood.* 2010;115(5):1062-9.
30. Lewandowska MA. The missing puzzle piece: splicing mutations. *Int J Clin Exp Pathol.* 2013;6(12):2675-82.
31. Vaz-Drago R, Custodio N, and Carmo-Fonseca M. Deep intronic mutations and human disease. *Hum Genet.* 2017;136(9):1093-111.
32. Delaunay J, Nouyrigat V, Proust A, Schischmanoff PO, Cynober T, Yvart J, et al. Different impacts of alleles alphaLEPRA and alphaLELY as assessed versus a novel, virtually null allele of the SPTA1 gene in trans. *Br J Haematol.* 2004;127(1):118-22.
33. Miraglia del Giudice E, Nobili B, Francese M, D'Urso L, Iolascon A, Eber S, et al. Clinical and molecular evaluation of non-dominant hereditary spherocytosis. *Br J Haematol.* 2001;112(1):42-7.
34. Dhermy D, Steen-Johnsen J, Bournier O, Hetet G, Cynober T, Tchernia G, et al. Coinheritance of two alpha-spectrin gene defects in a recessive spherocytosis family. *Clin Lab Haematol.* 2000;22(6):329-36.
35. Nussenzveig RH, Christensen RD, Prchal JT, Yaish HM, and Agarwal AM. Novel alpha-spectrin mutation in trans with alpha-spectrin causing severe neonatal jaundice from hereditary spherocytosis. *Neonatology.* 2014;106(4):355-7.
36. Singh RK, and Cooper TA. Pre-mRNA splicing in disease and therapeutics. *Trends Mol Med.* 2012;18(8):472-82.
37. Baralle D, and Buratti E. RNA splicing in human disease and in the clinic. *Clin Sci (Lond).* 2017;131(5):355-68.
38. Havens MA, Duelli DM, and Hastings ML. Targeting RNA splicing for disease therapy. *Wiley interdisciplinary reviews RNA.* 2013;4(3):247-66.
39. Marchesi SL, Knowles WJ, Morrow JS, Bologna M, and Marchesi VT. Abnormal spectrin in hereditary elliptocytosis. *Blood.* 1986;67(1):141-51.
40. Gallagher PG, Zhang Z, Morrow JS, and Forget BG. Mutation of a highly conserved isoleucine disrupts hydrophobic interactions in the alpha beta spectrin self-association binding site. *Lab Invest.* 2004;84(2):229-34.
41. Fairbanks G, Steck TL, and Wallach DF. Electrophoretic analysis of the major polypeptides of the human erythrocyte membrane. *Biochemistry.* 1971;10(13):2606-17.
42. Speicher DW, Morrow JS, Knowles WJ, and Marchesi VT. Identification of proteolytically resistant domains of human erythrocyte spectrin. *Proc Natl Acad Sci U S A.* 1980;77(10):5673-7.

43. Wang K, Li M, and Hakonarson H. ANNOVAR: functional annotation of genetic variants from high-throughput sequencing data. *Nucleic Acids Res.* 2010;38(16):e164.

44. Kircher M, Witten DM, Jain P, O'Roak BJ, Cooper GM, and Shendure J. A general framework for estimating the relative pathogenicity of human genetic variants. *Nat Genet.* 2014;46(3):310-5.

45. Schwarz JM, Rodelsperger C, Schuelke M, and Seelow D. MutationTaster evaluates disease-causing potential of sequence alterations. *Nat Methods.* 2010;7(8):575-6.

46. Li H, and Durbin R. Fast and accurate short read alignment with Burrows-Wheeler transform. *Bioinformatics.* 2009;25(14):1754-60.

47. DePristo MA, Banks E, Poplin R, Garimella KV, Maguire JR, Hartl C, et al. A framework for variation discovery and genotyping using next-generation DNA sequencing data. *Nat Genet.* 2011;43(5):491-8.

48. Ipsaro JJ, Harper SL, Messick TE, Marmorstein R, Mondragon A, and Speicher DW. Crystal structure and functional interpretation of the erythrocyte spectrin tetramerization domain complex. *Blood.* 2010;115(23):4843-52.

49. Harper SL, Sriswasdi S, Tang HY, Gaetani M, Gallagher PG, and Speicher DW. The common hereditary elliptocytosis-associated alpha-spectrin L260P mutation perturbs erythrocyte membranes by stabilizing spectrin in the closed dimer conformation. *Blood.* 2013;122(17):3045-53.

50. Sriswasdi S, Harper SL, Tang HY, Gallagher PG, and Speicher DW. Probing large conformational rearrangements in wild-type and mutant spectrin using structural mass spectrometry. *Proc Natl Acad Sci U S A.* 2014;111(5):1801-6.

51. Benjamini Y, and Hochberg Y. Controlling the False Discovery Rate: A Practical and Powerful Approach to Multiple Testing. *J Royal Statistical So Series B (Methodological).* 1995;57(1):289-300.

Figures

Figure 1. Haplotyping at the SPTA1 locus. Haplotype analysis around the *SPTA1* locus of all 71 alleles with the α^{BH} variant, Ala970Asp, in the 1000G2015 database and two rHS patients heterozygous for the α^{BH} variant. The α^{BH} allele is denoted in black and the rare intron 30 variant, the α^{LEPRA} allele, is denoted in blue. HG19 reference sequence is denoted in gray and non-reference sequence is shown in red. The *SPTA1* gene is shown below. Far left panel. Four individuals in the 1000G2015 database (green) and both rHS patients (red) carry the α^{LEPRA} allele.

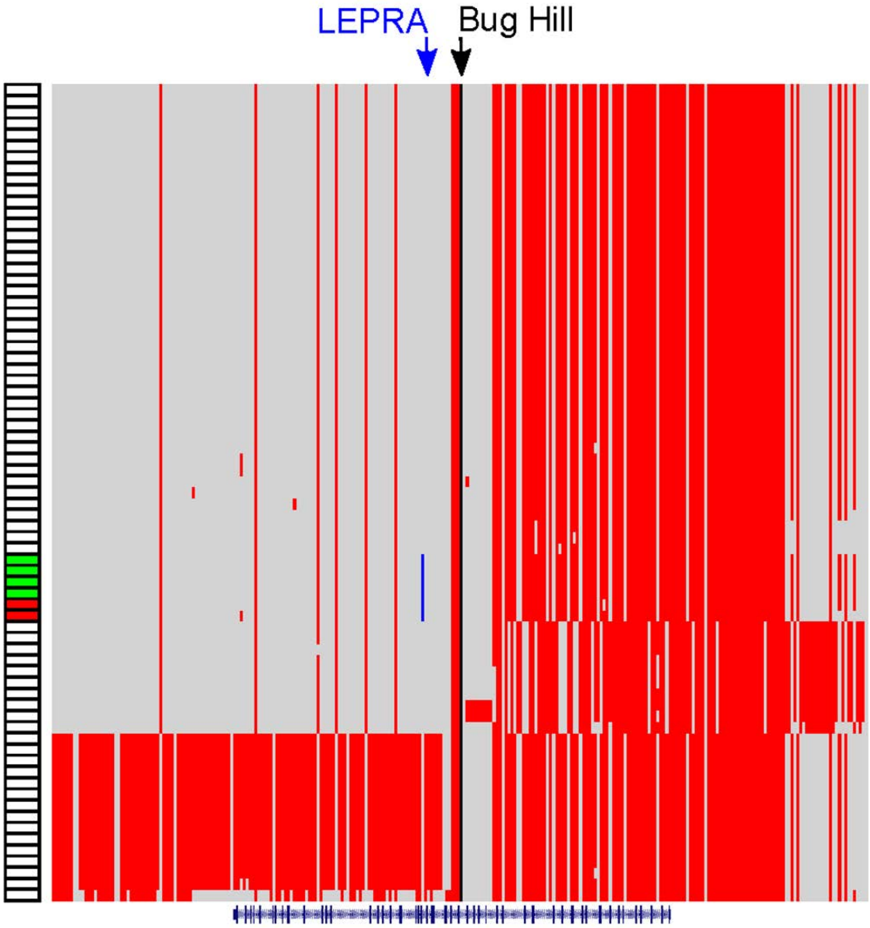

Figure 2. An elongated transcript of intron 30 of the SPTA1 gene. Top. Normalized RNA-seq profiles of the *SPTA1* intron 30 region in human wild type, primary erythroid cells and K562 cells are shown. Estimated percentages of elongated, partial intron 30-containing mRNA transcripts based on splice junction reads are shown. Bottom. A Sashimi plot demonstrates utilization of splice sites in intron-spanning reads.

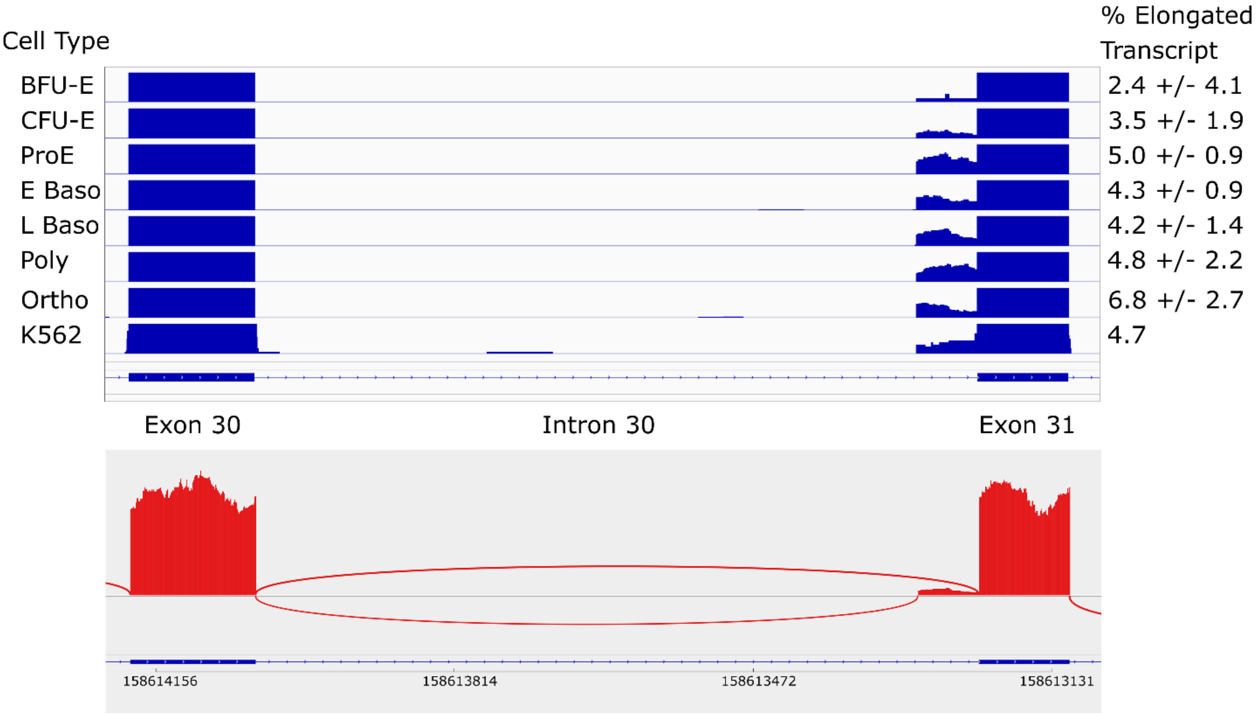

Figure 3. Computational analyses of intron 30 splicing of the human SPTA1 gene. A and B. A schematic of *cis* sequences and branch point (BP) usage in wild type (**A**) and α^{LEPRA} *SPTA1* alleles (**B**). In wild type cells, BP1 is primarily utilized, producing large amounts of correctly spliced, in frame mRNA transcripts (blue), while utilization of a weak, alternate BP2 leads to production of a small amount of elongated transcript that leads to frameshift and a novel termination codon (red). The α^{LEPRA} mutation, which changes BP2 from a weak alternate BP to a strong alternate BP, leads to increased utilization of BP2 producing large amounts of elongated transcript (red) with decreased utilization of BP1 leading to production of a small amount of correctly spliced transcript. (**C**). Branchpointer, an algorithm that predicts branch points, shows both BP1 and BP2-WT have low BP probability scores (0.51 and 0.67, respectively), while the α^{LEPRA} variant markedly improves the probability score of BP2-L (0.94). (**D**). These observations are true when comparing intron 30 BP probability scores to the predicted branch point probability scores of the BPs of 8180 introns of 1000 highly expressed erythroid genes.

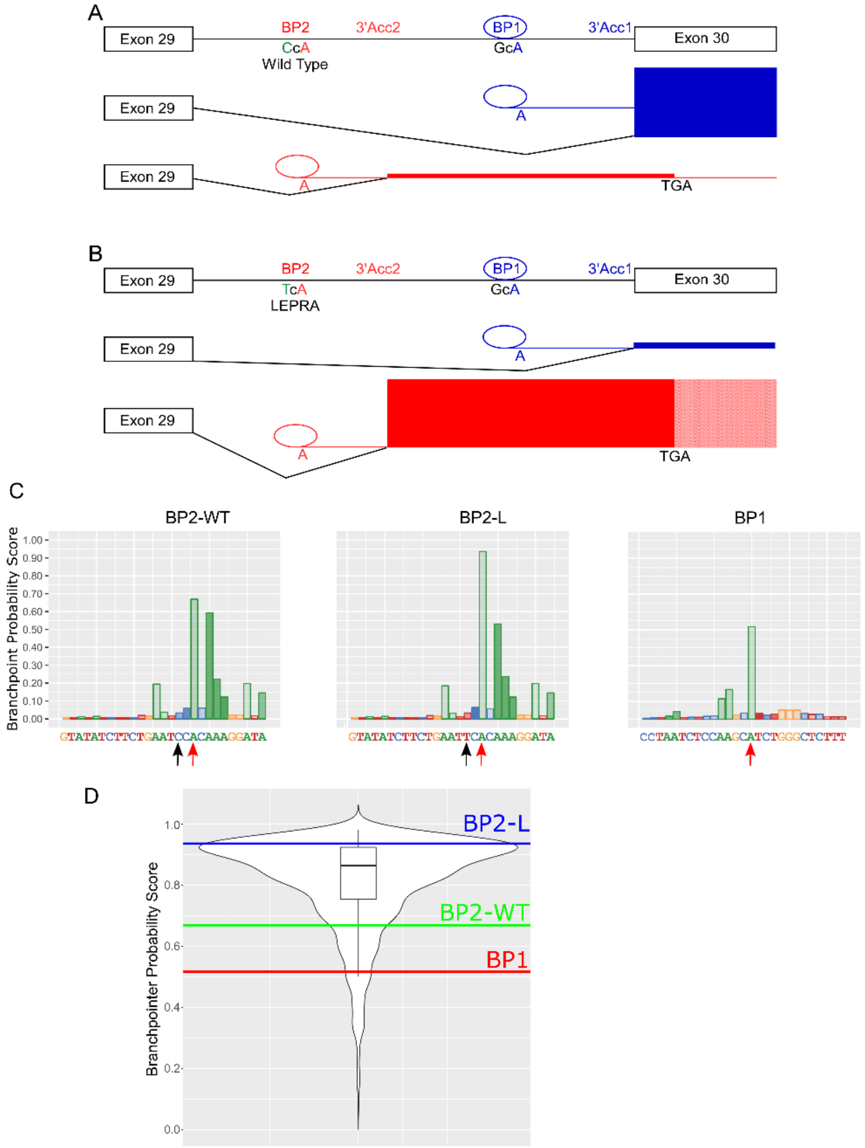

Figure 4. Minigene studies of α-spectrin intron 30 and the α^{LEPRA} variant. (**A**). Partial sequence of intron 30 of the *SPTA1* gene, showing the location of the α^{LEPRA} variant. (**B**). Each minigene construct used in minigene assays (Top) includes the *ANK1* erythroid promoter, a fragment of *SPTA1* genomic DNA inserted into intron 2 of the *HBG1* gene, and the *HBG1* 3'untranslated region and polyA signal. The hybrid *HBG1- SPTA1* transcripts derived from minigenes are shown, either wild type or elongated (Bottom), with the locations of Taqman probes utilized to detect total spectrin (T bar) or the unique insert of the elongated transcript (E bar). (**C**). Minigene results. The specific sequences utilized in minigene constructs are shown. Percentages of elongated α-spectrin transcript over total α-spectrin transcript are shown in the second column from right. The adjusted *p*-value of the difference from Wild Type is shown on the right.

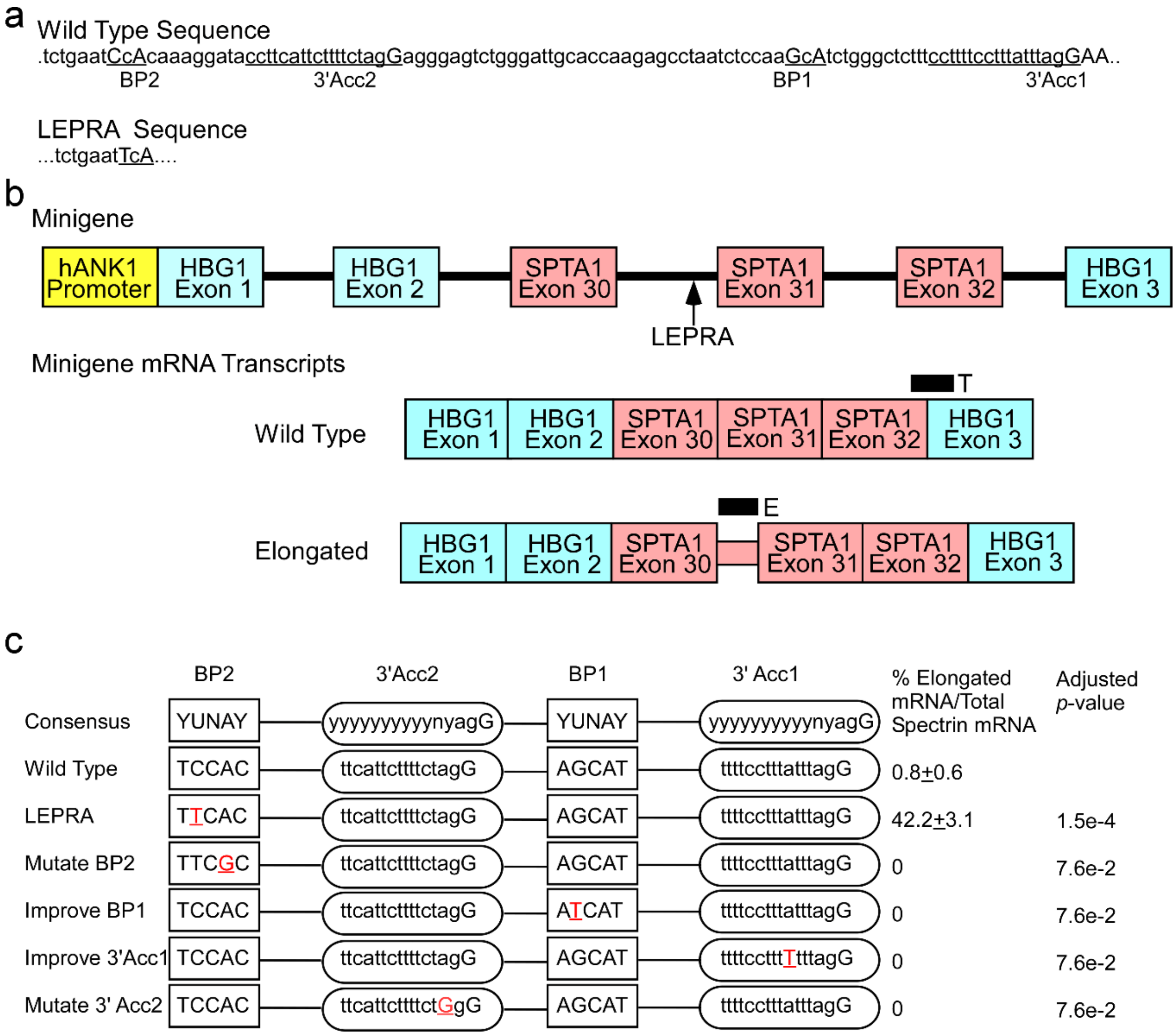

	BP2	3'Acc2	BP1	3' Acc1	% Elongated mRNA/Total Spectrin mRNA	Adjusted *p*-value
Consensus	YUNAY	yyyyyyyyyynyagG	YUNAY	yyyyyyyyyynyagG		
Wild Type	TCCAC	ttcattcttttctagG	AGCAT	ttttcctttatttagG	0.8±0.6	
LEPRA	TTCAC	ttcattcttttctagG	AGCAT	ttttcctttatttagG	42.2±3.1	1.5e-4
Mutate BP2	TTCGC	ttcattcttttctagG	AGCAT	ttttcctttatttagG	0	7.6e-2
Improve BP1	TCCAC	ttcattcttttctagG	ATCAT	ttttcctttatttagG	0	7.6e-2
Improve 3'Acc1	TCCAC	ttcattcttttctagG	AGCAT	ttttcctttTtttagG	0	7.6e-2
Mutate 3' Acc2	TCCAC	ttcattcttttctGgG	AGCAT	ttttcctttatttagG	0	7.6e-2

Figure 5. Analyses of nonsense mediated decay (NMD). The influence of nonsense mediated decay (NMD) on the stability of the elongated α-spectrin transcript in WT K562 cells and in K562 cells rendered homozygous for the α^{LEPRA} allele. (**A**). After treatment with the NMD inhibitor emetine (E) or cycloheximide (C), or both, the amounts of total a-spectrin and the elongated α-spectrin transcript were determined by real time RT-PCR with fluorescent Taqman probes. After NMD inhibition, amounts of elongated α-spectrin transcript were increased in α^{LEPRA} cells (adjusted *p*-values 0.0014, 0.0027 and 0.0014 for WT vs. cycloheximide, emetine and cycloheximide + emetine, respectively) and to a lesser extent in WT cells (adjusted *p*-values 0.084, 0.012, and 0.0047 respectively). (**B**). Minigene assay of NMD. Two nucleotides were inserted into the polypyrimidine tract of the primary 3'acceptor site of exon 30 in the minigene model to place the elongated transcript in-frame. As predicted, NMD was abrogated and the amounts of elongated α-spectrin transcript from both the WT and the α^{LEPRA} minigene constructs significantly increased. Three biologic samples each were tested in 3 independent experiments with the mean calculated from 9 values. Statistical significance was determined by two tailed Student's t test.

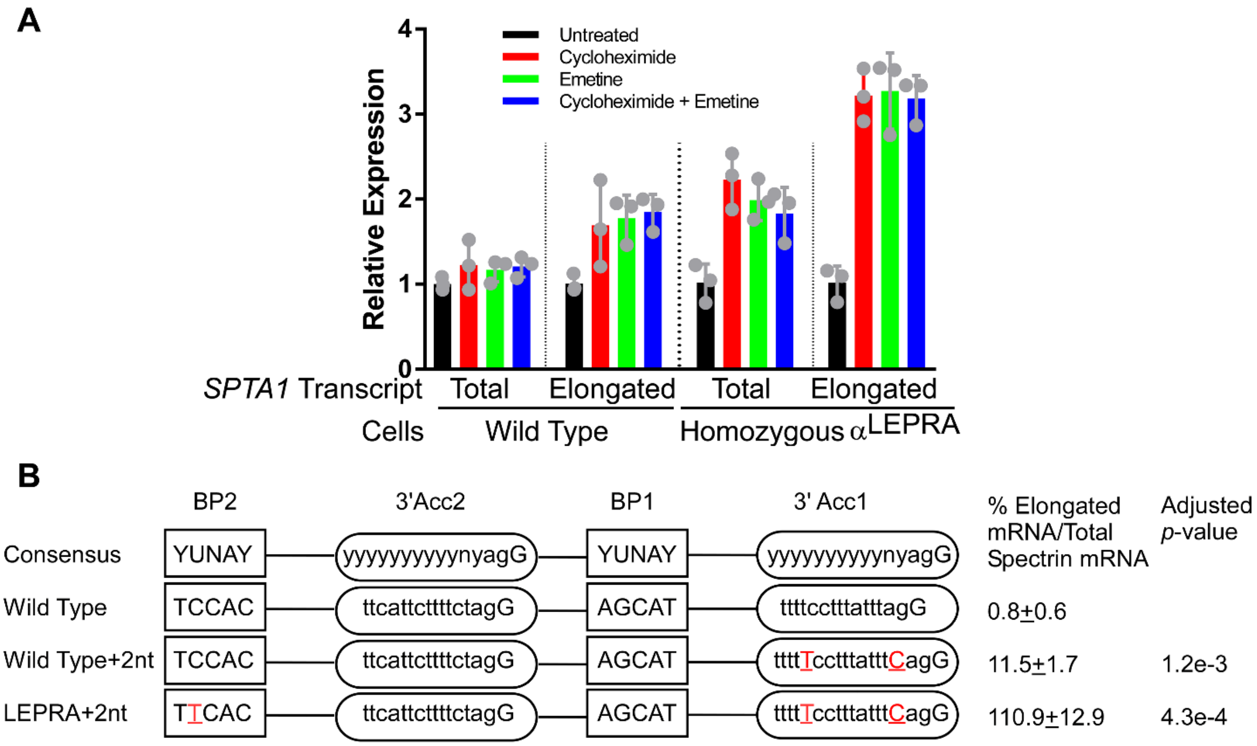

Table 1. Patient Diagnosis and Genetic Characteristics

Patient Number /Group	Diagnosis		Mutation Type	Mutation Location	Mutation	1000G[1]	ExAc[2]	CADD Phred[3]	Mutation Tester[4]
1/1	rHS	Allele 1	splicing	Intron 44	c.6418-1G>A	Not found	Not found	27.20	1.00
		Allele 2	splicing	Intron 30	c.4339-99C>T	0.000799	Not found	NA	NA
2/1	rHS	Allele 1	missense	Exon 2	c.209T>G:p.M70R	Not found	Not found	9.85	0.97
		Allele 2	missense	Exon 2	c.209T>G:p.M70R	Not found	Not found	9.85	0.97
3/1	rHS	Allele 1	splicing	Intron 30	c.4339-2A>C	Not found	8.40E-06	25.40	1.00
		Allele 2	missense	Exon 2	c.209T>G:p.M70R	Not found	Not found	9.85	0.97
4/1	rHS	Allele 1	nonsense	Exon 37	c.5203C>T:p.R1735*	Not found	Not found	37.00	1.00
		Allele 2	splicing	Intron 30	c.4339-99C>T	0.000799	Not found	NA	NA
5/1	rHS	Allele 1	nonsense	Exon 22	c.3139C>T:p.R1047*	Not found	Not found	35.00	1.00
		Allele2	splicing	Intron 30	c.4339-99C>T	0.000799	Not found	NA	NA
6/1	rHS	Allele 1	splicing	Intron 30	c.4339-99C>T	0.000799	Not found	NA	NA
		Allele 2	splicing	Intron 30	c.4339-99C>T	0.000799	Not found	NA	NA
7/1	rHS	Allele 1	splicing	Exon 4	c.531+1G>A	Not found	Not found	25.90	1.00
		Allele 2	splicing	Intron 30	c.4339-99C>T	0.000799	Not found	NA	NA
8/2	rHS	Allele 1	deletion	Exon 48	c.6756delG:p.M2252fs	Not found	Not found	NA	NA
		Allele 2	splicing	Intron 30	c.4339-99C>T	0.000799	Not found	NA	NA
9/2	rHS	Allele 1	nonsense	Exon 44	c.6335T>G:p.L2112*	Not found	Not found	46.00	1.00
		Allele 2	splicing	Intron 30	c.4339-99C>T	0.000799	Not found	NA	NA
10/2	rHS	Allele 1	nonsense	Exon 39	c.5530C>T:p.R1844*	Not found	Not found	39.00	1.00
		Allele 2	splicing	Intron 30	c.4339-99C>T	0.000799	Not found	NA	NA
11/2	rHS	Allele 1	splicing	Intron 37	c.5311-2A>G	Not found	Not found	24.80	1.00
		Allele 2	splicing	Intron 30	c.4339-99C>T	0.000799	Not found	NA	NA

12/2	HPP	Allele 1	insertion	Exon 4	c.460_461insTGC:p.L154insL	Not found	8.28E-06	NA	NA
		Allele 2	splicing	Intron 30	c.4339-99C>T	0.000799	Not found	NA	NA
13/2	HPP	Allele 1	missense	Exon 2[5]	c.83G>A:p.R28H	0.000399	2.49E-05	34.00	1.00
		Allele 2	splicing	Intron 30	c.4339-99C>T	0.000799	Not found	NA	NA
14/2	HPP	Allele 1	nonsense	Exon 41	c.5804G>A:p.W1935*	Not found	Not found	50.00	1.00
		Allele 2	splicing	Intron 30	c.4339-99C>T	0.000799	Not found	NA	NA
15/3	TD	Allele 1	deletion	Exon 52	c.7199delG:p.G2400fs	Not found	Not found	NA	NA
		Allele 2	nonsense	Exon 37	c.5215C>T:p.Q1739*	Not found	Not found	38.00	1.00
16/3	TD	Allele 1	nonsense	Exon 2	c.178C>T:p.R60*	Not found	8.31E-06	34.00	1.00
		Allele 2	nonsense	Exon 41	c.5804G>A:p.W1935*	Not found	Not found	50.00	1.00
17/3	TD	Allele 1	nonsense	Exon 31	c.4398T>G:p.Y1466*	Not found	Not found	42.00	1.00
		Allele 2	splicing	Intron 30	c.4339-99C>T	0.000799	Not found	NA	NA
18/3	TD	Allele 1	deletion	Exon 41	c.5814delT:p.D1938fs	Not found	Not found	NA	NA
		Allele 2	missense	Exon 8	c.1037A>G:p.E346G	Not found	Not found	22.70	0.84
19/3	TD	Allele 1	nonsense	Exon 36	c.5102T>A:p.L1701*	Not found	Not found	43.00	1.00
		Allele 2	missense	Exon 6	c.803G>A:p.R268Q	Not found	Not found	28.00	1.00
20/3	TD	Allele 1	missense	Exon 2	c.146T>G:p.L49R	Not found	Not found	28.50	1.00
		Allele 2	splicing	Intron 45	c.6531-12C>T	0.227835	0.2564	NA	NA
21/3	TD	Allele 1	missense	Exon 2	c.133A>G:p.R45G	Not found	Not found	25.90	1.00
		Allele 2	missense	Exon 2	c.133A>G:p.R45G	Not found	Not found	25.90	1.00
22/3	TD	Allele 1	nonsense	Exon 27	c.3823C>T:p.Q1275*	Not found	Not found	35.00	1.00
		Allele 2	missense	Exon 2[5]	c.83G>A:p.R28H	0.000399	2.49E-05	34.00	1.00
23/3	TD	Allele 1	nonsense	Exon 23	c.3267T>A:p.Y1089*	Not found	Not found	40.00	1.00
		Allele 2	splicing	Intron 30	c.4339-99C>T	0.000799	Not found	NA	NA

24/3	TD	Allele 1	deletion		c.340delA:p.Thr114Glnfs	Not found	Not found	NA	NA
		Allele 2	splicing	Intron 30	c.4339-99C>T	0.000799	Not found	NA	NA

(Legend. Abbreviations: rHS: recessive hereditary spherocytosis; HPP: hereditary pyropoikilocytosis; NA: not available. [1]1000G: frequency in 1000 Genomes Database. [2]ExAc: frequency in Exome Aggregation Consortium (ExAc) database. [3]CADD Phred: predicted score of the deleteriousness of mutations by the Combined Annotation Dependent Depletion (CADD) algorithm. [4]Mutation Taster: score of the disease-causing potential of DNA variants. [5]Previously reported.(1-3)